

The Study of Continuum-particle hybrid coupling for mass and energy transfers in unsteady fluid flow

Dr. Shashi Sekhar Vidyarthi ^{*1}, Ajay Kumar²

^{1*}Department of Physics, JLN College Dehri-on-Sone V.K.S. University, Ara. India

²Department of Physics M.U. Bodhgaya, Bihar, India

ABSTRACT

The aim of hybrid methods in simulations is to communicate regions with disparate time and length scales. In this case, an inner area P with atomistic fluid description and an outer region C with continuum fluid dynamics description are connected. Over an overlapping region, the two descriptions of matter are matched. Consists of a two-way coupling system (C→P and P→C) that transmits fluxes of mass, momentum, and energy. The hybrid system that is given here makes two contributions. It first deals with erratic flows and, more crucially, with energy transfer between the C and P areas. Using stable and unsteady flows with various rates of mass, momentum, and energy exchange, the C→P coupling is evaluated here. Since they include all hydrodynamic modes, relaxing flows represented by linear hydrodynamics—including transverse and longitudinal waves—are the most illuminating. The cell-averaged Fourier components of the flow variables in the P region—velocity, density, internal energy, temperature, and pressure—evolve in excellent agreement with the hydrodynamic trends when the hybrid coupling scheme is used following the commencement of an initial disturbance. Additionally, it is demonstrated that the method maintains the proper rate of entropy creation. We go through some broad specifications for the coarse-grained length and temporal scales that result from the distinctive microscopic and hydrodynamic scales.

Keywords: coupling system, particle dynamics, fluid phase

INTRODUCTION

A fine interaction between the slow dynamics in the system's bulk and the atomistic processes that take place in a tiny portion of the system governs a broad variety of systems with significant applications. Polymers or colloids at surfaces, wetting, drop formation, melting, crystal development from a fluid phase, and moving interfaces of immiscible fluids or membranes are only a few examples of the numerous instances that emerge in complex flows near interfaces. Such studies call for new algorithms that can maintain the benefits of the atomistic description of matter where it is really needed while treating the majority of the system by much less expensive continuum fluids because the computational cost of realistic-size simulations of these problems via standard molecular dynamics (MD) is prohibitive. In recent literature, a number of hybrid

algorithms of this type have been presented. These hybrid systems often combine the particle region P and the continuum region C via an overlapping region made up of the two buffers $C \rightarrow P$ and $P \rightarrow C$, which take into consideration the two-way transmission of information from C to P . With just the restricted prescription from the C area as input, one must rebuild the dynamics of a huge collection of particles at $C \rightarrow P$, whereas the $P \rightarrow C$ transfer effectively entails a coarse-graining technique. Additionally, it is important to incorporate as few non-physical artifacts—such as Maxwell demons—as feasible when completing this reconstruction. The essential component of any hybrid design, this Endeavour is quite challenging. Fluids hybrid algorithms are a relatively new development. The elegant technique for rarefied gases developed by Garcia et al. [1] connects fluxes from a direct simulation Monte Carlo (DSMC) scheme to a different area that is characterized by computational fluid dynamics (CFD). An adaptive mesh refinement hierarchy is utilized, with a CFD semi-implicit solver being used at the finer grid sizes. The DSMC is established at these scales. An MD-continuum liquid description may theoretically be used to construct the scheme, but in that case the C solver would have to be entirely explicit to prevent having to modify the particle's energy during the iterations of the implicit scheme. Due to the challenges brought on by the inter particle interactions, the state of the art is comparatively less developed when it comes to liquids. O'Connell and Thompson's groundbreaking work [2] linked momentum by imposing the local continuum velocity at $C \rightarrow P$ through an unrefined restriction. Dynamic Lagrangian theory. The P region in this illustration is close to a physical surface that is depicted by the rightmost shaded area. At some distance from the surface, the continuum zone extends into the area to the left. In the overlapped region, particle-averaged fluxes are introduced into the C flow in a $P \rightarrow C$ cell and the C flow is conveyed to P in a $C \rightarrow P$ cell. The control cells of the C solver are indicated by dashed lines, with area A and grid spacing DX . A cell's centre, as well as its west and east surfaces, are denoted by the letters O , W , and E , respectively. The main cell's vectors (\mathbf{n}_W , \mathbf{n}_E , and \mathbf{n}_{PC}) have been indicated. Hadji Constantine and Patera [3] introduced a reservoir region to impose boundary conditions on the P region. Particles were assigned a velocity while residing in the reservoir that was taken from a Maxwellian distribution with a mean and variance that matched the speed and temperature of the C flow at each time step. The authors smoothed the field variables produced from P at the $P \rightarrow C$ area using a low order polynomial in order to achieve the boundary condition for the C region. The boundary conditions for the P and C areas must coincide. A Schwarz alternating method-based iterative technique was implemented that is appropriate for continuous incompressible flows. Liao and colleagues [4] suggested an advanced technique. When the flow exhibits significant gradients, this concept may be employed to reduce the $P \rightarrow C$ coupling, however at a significant computational expense. Liao and colleagues [4] introduced a novel Maxwell demon termed the reflecting particle technique to transmit momentum on the P area. The pressure gradient becomes an output rather than an input of the simulation, which is a disadvantage. Finally, Flekkoy et al. [5] incorporated mass transfer in addition to coupling through fluxes. Energy transfer was still prohibited, and only steady flows were taken into account. The primary goal of the current research is to widen the applicability of such hybrid schemes in order to

provide a more comprehensive description that allows mass, momentum, and energy coupling in unstable flows. Determining the type of information that has to be conveyed at C→P and P→C is a key issue. There are essentially two ways to transfer generalized forces: either local values of the averaged variables or fluxes of conserved quantities. The published literature has examples of both types of techniques. Here, in the context of energy transfer, we demonstrate that coupling through fluxes is required since imposing the local C values at the border of P under unstable flows is insufficient. Flux coupling may also have the advantage of avoiding the difficulties associated with dealing with fluids whose constitutive relations are unknown or only partially known, according to Flekkoy et al. [5]. We demonstrate that even while we concur that the flux-based coupling is the proper matching method, the hybrid strategy fails to link the time evolution of both domains if the transport coefficients at C and P are sufficiently different. Therefore, in these situations, it is necessary for the hybrid scheme to function properly to evaluate the transport coefficients using normal microscopic techniques, at least for the range of densities and temperatures under consideration. The remainder of the essay is organized as follows. In Section II, the equations controlling the continuum and particle areas as well as the averaging techniques are provided. Sec. III presents the main ideas of the scheme, which describe the C→P coupling for momentum, energy, and mass fluxes. In Section IV, general criteria for the coarse-graining length and time scales are covered. The unstable flows where the plan has been tried. The particle region P and the continuum region C need to be differentiated from one another. A group of particles called Region P interact through predetermined interparticle potentials and move through time according to Newtonian dynamics. The coupling process will be demonstrated by using a Lennard-Jones LJ fluid. There are N(t) particles in P.

$$\dot{\mathbf{r}}_i = \mathbf{v}_i,$$

$$m \dot{\mathbf{v}}_i = \mathbf{f}_i = \sum_{j=1}^N \frac{d\psi(r_{ij})}{dr_{ij}} \frac{\mathbf{r}_{ij}}{r_{ij}}, \dots\dots\dots [1,2]$$

$$\frac{\partial \rho}{\partial t} = - \nabla \cdot \rho \mathbf{u}, \tag{3}$$

$$\frac{\partial \mathbf{j}}{\partial t} = - \nabla \cdot (\mathbf{j} \mathbf{u} + \mathbf{\Pi}), \tag{4}$$

$$\frac{\partial \rho e}{\partial t} = - \nabla \cdot (\rho e \mathbf{u} + \mathbf{\Pi} \cdot \mathbf{u} + \mathbf{q}), \tag{5}$$

where the specific energy $e = u^2/2 + 3T/2 + \phi$ includes the translational energy, the thermal kinetic energy, and the potential energy ϕ . The momentum flow contains contributions from convection $\mathbf{j}u$ and the pressure tensor $\Pi = P\mathbf{1} + \tau$, the latter including the local hydrostatic pressure $P(\mathbf{R}, t)$, the viscous stress tensor, which satisfy a Newtonian constitutive relation, as shown by previous MD descriptions of the LJ fluid.

$$\tau = -\eta \left(\nabla \mathbf{u} + (\nabla \mathbf{u})^T - \frac{2}{3} \nabla \cdot \mathbf{u} \right) - \xi \nabla \cdot \mathbf{u}. \quad (6)$$

The energy current includes convection $\rho e \mathbf{u}$, dissipation $\Pi \mathbf{u}$ and conduction \mathbf{q} , which can be expressed in terms of the local temperature gradients and the thermal conductivity k_c , through Fourier's law $\mathbf{q} = -k_c \nabla T(\mathbf{R}, t)$. Knowing the caloric $e(\rho, T)$ and thermal equations of state $P(\rho, T)$, as well as the constitutive relations for the transport coefficients shear and bulk viscosities and thermal conductivity; η , ξ , and k_c , respectively! in terms of a set of independent thermodynamic variables, such as ρ and T , is required in order to solve the aforementioned equations. The transport coefficients η , k_c , and ξ were taken from Heyes [7] and Borgelt et al. [8] and the equations of state for a LJ fluid were taken from Johnson et al. [6]. The slower variables are those that are important to the C area. Using any well used solver for continuum fluid dynamics.

AVERAGES:

For information to be transferred from the quicker time-scale and shorter length-scale particle dynamics to the slower and longer coarse-grained description, averages are required. Averages must be local on the slower time scale and in the coarse-grained spatial coordinates to handle unsettled, no equilibrium conditions. We define the following averages for any particle variable, let's say ϕ_i :

$$\bar{\Phi}(\mathbf{R}_l, t) \equiv \frac{1}{N_l} \sum_{i \in V_l}^{N_l} \phi_i, \quad (7)$$

$$\langle \bar{\Phi} \rangle(\mathbf{R}_l, t_C) \equiv \frac{1}{\Delta t_C} \int_{t_C}^{t_C + \Delta t_C} \bar{\Phi}(\mathbf{R}_l, t) dt, \quad (8)$$

Where the summation in Eq. [7] is made over the N_l particle inside the cell l . The averaging procedure is needed to translate the P and C “languages” to and from each domain. This translation is done within the overlapping region, where the two descriptions of matter coexist ~ In particular, within the $P \rightarrow C$ cells, the many degrees of freedom arising from the particle dynamics are coarse grained to provide boundary conditions at the “upper” C-level. As long as

the number of degrees of freedom is very much larger at P than at C , this operation is rather straightforward and is based on the microscopic derivation of continuum fluid dynamics [9]

$$\rho \mathbf{u} \cdot \mathbf{n}_{PC} = \frac{1}{V_{PC}} \left\langle \sum_{i=1}^{N_{PC}} m \mathbf{v}_i \right\rangle \cdot \mathbf{n}_{PC}, \quad (9)$$

$$\mathbf{\Pi} \cdot \mathbf{n}_{PC} = \frac{1}{V_{PC}} \left\langle \left(\sum_{i=1}^{N_{PC}} m \mathbf{v}_i \mathbf{v}_i - \frac{1}{2} \sum_{i,j}^{N_{PC}} \mathbf{r}_{ij} \mathbf{F}_{ij} \right) \right\rangle \cdot \mathbf{n}_{PC}, \quad (10)$$

$$\mathbf{q} \cdot \mathbf{n}_{PC} = \frac{1}{V_{PC}} \left\langle \left(\sum_{i=1}^{N_{PC}} m \epsilon_i \mathbf{v}_i - \frac{1}{2} \sum_{i,j}^{N_{PC}} \mathbf{r}_{ij} \mathbf{v}_i \mathbf{F}_{ij} \right) \right\rangle \cdot \mathbf{n}_{PC}, \quad (11)$$

Where N_{PC} is the number of particles inside the P/C cell and \mathbf{n}_{PC} is the surface vector shown, By contrast, within the C/P cells, the particle dynamics must be modified to conform to the averaged-dynamics prescribed by the continuum description. In other words, one needs to construct a sort of “generalized boundary condition” for the particle dynamics. As pointed out in all previous papers on the subject [1–3,], this represents the most demanding challenge in that one needs to *invent* a way to reconstruct the microscopic dynamics of a large number of particles, based on only a few properties of the local continuum variables. Moreover, to ensure that the effect on the inner P region is minimized, it is crucial to reduce as much as possible the unphysical artifacts, such as Maxwell demons, which are added to the particle dynamics at $C \rightarrow P$. The present work is focused on this problem, which lies at the core of any hybrid scheme.

THE CP COUPLING

This part of the hybrid scheme can be alternatively stated as the imposition of generalized ~mass, momentum, and energy boundary conditions on an MD simulation box. To deal, with this task we have coupled the particle region to a collection of flows ~with explicit analytical solution!, which involves the whole set of conserved quantities exchanged, ~mass, momentum, and energy!. In this sense, in the present work our C -solver is not numerical but rather analytical. In particular, we use the initial no equilibrium state imposed at P to calculate the time-dependent analytical solution at C . This C -flow is then imposed on the P region during the rest of the simulation, meaning that apart from the initial state the hybrid coupling used in the tests presented here works in one direction only ~from C to P).\

HYDRODYNAMIC MODES

Our hybrid approach has been tested with both stationary and erratic flows, as was already described. We took into account common stationary nonequilibrium states such Couette profiles [13] and heat conduction profiles [13]. Nothing new needs to be said because the microscopic

reconstruction of these flows has been well researched in the literature. In passing, we mention that the diffusive times L_x/k and L_x/n were found to be in accord with the transient periods to attain the steady state from the rest solution. The remainder of the conversation will concentrate on our selection of unstable circumstances. They are modeled by the transverse and longitudinal wave decay. Now, a brief presentation of these flows using conventional hydrodynamics is given. Think about a fluid that is in equilibrium and has the following properties: homogenous mass density ρ_e , specific energy e_e , and vanishing mean velocity $u_e=0$. Our method involves perturbing this equilibrium state with various hydrodynamic fields and then using the C→P coupling technique outlined in Sec. III to check that the ensuing evolution towards equilibrium is carried out inside the particle area in a hydro dynamically consistent manner. If the liberalized mass, momentum, and energy equations (3-5) [14] are to always dominate the relaxation process, then the externally caused perturbations must be minimal enough to ensure that the liberalized hydrodynamic theory may be used. We note that instead of using ep , the energy equation is expressed in terms of temperature fluctuations. Also, for clarity, it is better to write the solution \hat{F} in terms of the $t=0$ Fourier-transformed perturbative heat density Q_p and pressure P_p . These quantities are related to r_p and T_p through the relations.

$$\Phi(\mathbf{k}, t) \equiv \int_{-\infty}^{\infty} \Phi(\mathbf{r}, t) \exp(-i\mathbf{k} \cdot \mathbf{r}) d\mathbf{r},$$

$$\hat{\Phi}(\mathbf{k}, z) \equiv \int_0^{\infty} dz \exp(izt) \Phi(\mathbf{k}, t) dt.$$

RESULTS

The arrangement depicted in Fig. 3 was used to implement and test the coupling strategy. The gradients of the continuum variables are set along the x direction, and the system is periodic in the y and z directions. The particle region is located in an area with a size of $L_y=L_z$ along the periodic directions and L_x approximately $x=0$. To take local averages, the P area is split into control cells of size DX . The two C→P slabs' centers, or the outermost cells, are located at $x=\pm(L_x-X/2)$. The relative difference of the cell-averaged pressure and energy with regard to the values supplied by the Johnson et al. equation of state was used to measure the divergence from the local equilibrium assumption. Around a distance $1.5s$ away from the C→P interface, the typical maximum deviations were only about 6%. The initial perturbative flow was prepared by first letting the P region relax until a vanishing and homogeneous mean flow was obtained. Then, during a small time interval (3τ), the particle velocities were periodically changed according to a Maxwellian distribution with the desired velocity profile and local cell temperature. The resulting initial state was then analyzed to extract the Fourier components of the whole set of flow variables ($\mathbf{v}, \rho, T, e, P$). For the sake of consistency these were extracted by Fourier transforms of the cell-averaged variables,

$$\overline{\phi}_{\cos}^{(n)}(t) \equiv \frac{c_n}{M_c} \sum_I^{M_c} \overline{\phi}(X_I, t) \cos(k_n X_I),$$

$$\overline{\phi}_{\sin}^{(n)}(t) \equiv \frac{c_n}{M_c} \sum_I^{M_c} \overline{\phi}(X_I, t) \sin(k_n X_I),$$

where $kn=nk$ ($n=N$); and $cn=1$ for $n=0$, and $cn=2$ otherwise. In any case, it was checked that the Fourier transform of the microscopic variables $f(n)=cn(I Nf(xi ,t) 3exp(2iknxi)/N$ yields essentially the same output. To determine the temporal evolution of the continuum variables, the initial Fourier transforms obtained from Equations. The fluxes exerted on the C→P cells over time were then determined using these. The literature [7,6] reported the transport coefficients that were employed. An intriguing test revealed that the coupling strategy dramatically failed if the transport coefficients utilized in the C area deviated from those of the LJ fluid by more than roughly 15%. In particular, the averaged particle velocity oscillated at a different frequency than that of C, and correlations degenerated more quickly than in the case of the C flow. Because of this, before using the hybrid scheme in situations where the constitutive relations are unknown, it is first necessary to measure the transport coefficients from the particle dynamics using any common molecular technique, especially if unsteady flows are to be investigated. In order to operate inside the hydrodynamic regime, the wavelengths of the initial perturbations were selected to be much bigger than the mean free path, i.e., $2\pi\lambda/k < 1$. In other words, there was very little wave number dependency on the transport coefficients. The amplitudes of the initial perturbation were chosen small enough to ensure that the subsequent relaxation process could be described by the linear theory. In particular, if $v^-(1)(t)$ is the maximum Fourier amplitude of the velocity, the typical values of the Reynolds number at $t50$ [$Re=uv^-(kn)]\rho e / (kn)\#$ were $Re(0) < 3$. As $uv^{-(1)}(t)u$ decays exponentially, convection was present only in the first stages of the relaxing flow, but it was not strong enough to produce significant deviations from the linear theory .nonlinear effects become dominant for $Re.>O(10)$ [15].. The maximum Mach number was less than 0.2, and density fluctuations were around $\rho^{- (1)} / \rho e; Ma^2.=0.05$. In another test, the hybrid scheme was applied to a fluid in mechanical ($u50$) and thermodynamically equilibrium ($\rho= 0.5, T=3.5, e=2.7, P=3.2$) during a longer simulation (50τ) to check for any possible spurious drift in the overall momentum and energy note that Eq.15 ensures the mass conservation by construction#. During this calculation, the total momentum inside the P region was conserved up to, and the total energy fluctuated 5% around its equilibrium value. The size of these fluctuations is consistent with the system size ~which contained $N=1600$ particles and a specific heat of $cv51.8$). Note that the total energy of the system cannot be conserved because a part of the system is connected to a thermostat, and it also receives mechanical energy from C.

Mass

The fact that one can only theoretically exchange an integer number of particles, despite the continuum flux being a floating point value, is one of the primary issues with the hybrid mass transfer at C!P. The following steps are taken throughout each interval to ensure that the

continuum mass flow is maintained as nearly as possible: $t_C, t < t_C + \Delta t_C$, mPN . The first one evaluates the quantity

$$\xi(t_C) \equiv \int_{t_C}^{t_C + \Delta t_C} s(t) dt.$$

This floating point number, which represents the number of particles that should cross the C/P interface along $t_C, t < t_C + \Delta t_C$ is converted into an integer $dN(t)$ by the following construction

$$\begin{aligned} \delta N(t) &= NINT[\xi(t_C)] + \delta \xi(t - t_k), \\ \delta \xi(t - t_k) &= INT \left[\int_{t_k}^{t - \Delta t_P} [\xi(t') - \delta N(t')] dt' \right], \end{aligned}$$

Where t_k is such that $\delta \xi(t - t_k) < 1$ and $0 = t_0 < t_k < t_{k+1}$. The deviation $\delta \xi(t - t_k)$ assimilates the errors made through successive rounding off ($\xi \rightarrow NINT[\xi]$). When $\delta \xi(t - t_k)$ becomes larger than 1 (at $t = t_k$), a particle is added to ~or extracted from! dN and the corrector d_j is then reset to zero. To minimize the effect on the remaining particles over each interval Δt_C , the particle crossings are regularly separated in time at a rate as close as possible to $\delta N(t_C)/\Delta t_C$. As illustrated in Fig. 1, this kind of procedure enables us to follow rather closely the desired mass flux.

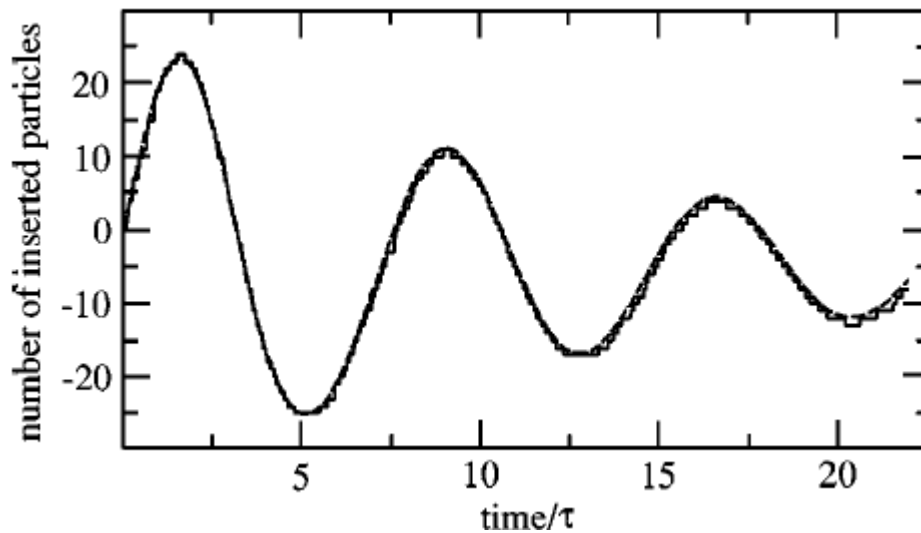


FIG. 1. The total number of inserted particles integration $dN(t)/dt$ at the rightmost $C \rightarrow P$ cell, along a simulation of a longitudinal wave with $k=0.168$ inside a region. The initial perturbative velocity profile was $u_x=0.60 \cos(kx)$. The dashed line is the continuum prescription, Time has been non dimensional with $t=(\sigma 2m/e)1/2$.

CONCLUSIONS

We have presented the core of a hybrid continuum particle method for fluids at moderate-to-large densities which couples mass, momentum, and energy transfers between two regions, C and P , described respectively by continuum fluid dynamics and by discrete particle Newtonian

dynamics. Both domains overlap within a coupling region divided into two sub cells which account for the two-way exchange: $C \rightarrow P$ and $P \rightarrow C$. While the procedure at the $P \rightarrow C$ cell is simply to average the particle-based mass, momentum, and energy fluxes in order to supply open boundary conditions to the C domain, the operations at the $C \rightarrow P$ cell are much less straightforward as they need to reconstruct a large number of particles' degrees of freedom only from the knowledge of the three fluxes of conserved quantities arising within C . The present work has been concerned with extending the $C \rightarrow P$ coupling to arbitrary rates of mass, momentum, and energy transfer. To this end, the proposed method has been tested under unsteady flows which demand conformance to the whole set of conserved variable densities. In particular, we have considered the set of relaxing flows arising from hydrodynamics, namely longitudinal and transversal waves. We have followed the idea proposed by Flekkoy *et al.* [5], in the sense that the scheme is explicitly based on direct flux exchange between the C and P regions. In order to deal with unsteady scenarios, we have shown that the fluxes injected into the particle region from the continuum region need to be measured exactly at the $C \rightarrow P$ interface and not at the nodes of the continuum lattice. The implementation of flux exchanges requires the supply of energy currents to the particle system arising from the C domain due to advection, dissipation, and conduction. To inject the correct amount of advected energy, the particle-averaged specific energy at the $C \rightarrow P$ cell needs to be equal to the continuum value. This can only be achieved if the new inserted particles are placed at positions where the interparticle potential energy equals the C -specified internal energy per unit mass. This severe condition has been implemented by the USHER algorithm, whose purpose is twofold: to provide the correct mass transfer rate and to ensure the balance of energy advection. In the proposed scheme, the balance of energy dissipation arises naturally, provided that the cell-averaged velocity and the injected momentum flux equal their continuum counterparts. This is made possible by applying the external force according to a flat distribution, instead of a biased one as used by Flekkoy *et al.* but as a result, the new particles have to be inserted within a non-vanishing density environment. This is sorted out by the USHER in a very efficient way. Energy conduction has been implemented by using a set of Nose-Hoover thermostats adjacent to the $C \rightarrow P$ interface, whose temperature and position are determined through the continuum local temperature gradient. Confirmation of the validity of this procedure is obtained from the correct rate of entropy production computed in our simulations of longitudinal waves. We showed that using only one thermostat per $C \rightarrow P$ cell—i.e., providing only the local value of T but not the heat flux—leads to negative entropy production. Therefore, in the context of energy transfer, this result reinforces the central importance of coupling through fluxes proposed by Flekkoy *et al.* Investigations into improving the current plan warrant some debate here. A feedback mechanism that maintains the momentum flux balance may be used to regulate the number density at $C \rightarrow P$. It is also important to think about different implementations for the conduction of energy. Last but not least, we intend to put the $P \rightarrow C$ coupling into practice alongside a 3D finite volume CFD solver. There will be some further challenges to overcome in order to expand the coupling technique to higher dimensions. The first step is to assign a mass flow to each cell in a cluster of

nearby C→P cells. Particles will therefore need to be put into precisely specified finite zones, and the insertion procedure could have to make a sacrifice to maintain mass continuity. In order to do this, it might be required to interpolate the external force along nearby C→P cells while still maintaining the local momentum flux imposed at each C→P cell. Similar to how the Maxwell distribution used here to determine the velocities of the new particles proved sufficient to guarantee momentum continuity for 1D coupling, i.e., with no neighboring C!P cells!, it may be convenient to use a Chapman-Enskog distribution in higher dimensions. The average velocity of the inserted particles can now conform to the velocity gradient along nearby C→P cells thanks to the latter distribution.

REFERENCES

- [1] A. Garcia, J. Bell, Wm.Y. Crutchfield, and B. Alder, *J. Comput.Phys.* **154**, 134 ~1999
- [2] S.T. O'Connell and P.A. Thompson, *Phys. Rev. E* **52**, R5792~1995
- [3] N. Hadjiconstantinou and A. Patera, *Int. J. Mod. Phys. C* **8**,967 ~1997 N.G. Hadjicostantinou, *Phys. Rev. E* **59**, 2475~1999
- [4] J. Li, D. Liao, and S. Yip, *Phys. Rev. E* **57**, 7259 ~1998
- [5] E.G. Flekkoy, G.Wagner, and J. Feder, *Europhys. Lett.* **52**, 271~2000
- [6] K. Johnson, J.A. Zollweg, and K.E. Gubbins, *Mol. Phys.* **78**,591 ~1993
- [7] D.M. Heyes, *Chem. Phys. Lett.* **153**, 319 ~1988
- [8] P. Borgelt, C. Hoheisel, and G. Stell, *Phys. Rev. A* **42**, 789~1990
- [9] D.J. Evans and G.P. Morris, *Statistical Mechanics of Nonequilibrium Liquids* ~Academic Press, London, 1990
- [10] Frenkel and B. Smith, *Understanding Molecular Simulations*~Academic Press, London, 1996
- [11] R. Delgado-Buscalioni and P.V. Coveney, *J. Chem. Phys.*
- [12] After submission but prior to publication of this paper we have implemented further improvement in the USHER algorithm. The new USHER scheme, to appear in Ref. 11, reduces the number of iterations to 8–30 for densities within the range $r_0=0.5-0.8$.
- [13] C. Trozzi and G. Ciccotti, *Phys. Rev. A* **29**, 916 ~1984!; A.Tenenbaum, G. Ciccotti, and Renato Gallico, *ibid.* **25**, 2778~1982
- [14] J.P. Hansen and I.R. McDonald, *Theory of Simple Liquids*~Academic Press, London, 1986
- [15] D.J. Tritton, *Physical Fluid Dynamics* ~Oxford University Press, Oxford, 1988